Unique Ultralow 18 pi-Trannulenyl HOMO-LUMO Energy Gap of Photostable Emerald-Green D-3d-2-Methylmalonato[60]fullerenes

ARTICLE *in* JOURNAL OF PHYSICAL CHEMISTRY LETTERS · AUGUST 2011

Impact Factor: 7.46 · DOI: 10.1021/jz200978f

Unique Ultralow 18π-Trannulenyl HOMO–LUMO Energy Gap of Photostable Emerald-Green D_{3d}-2-Methylmalonato[60]fullerenes

Alexey A. Popov,*[,†,§] Seaho Jeon,[‡] Vladimir M. Senyavin,[†] Lothar Dunsch,[§] Satyanarayana Maragani,[‡] Min Wang,[‡] Loon-Seng Tan,[¥] and Long Y. Chiang*[,‡]

[†] Department of Chemistry, Moscow State University, Moscow 119992, Russia

[‡] Department of Chemistry, Institute of Nanoscience and Engineering Technology, University of Massachusetts, Lowell, MA 01854, USA

[§] Leibniz Institute for Solid State and Materials research, IFW Dresden, 01069 Dresden, Germany

[¥] AFRL/RXBN, Air Force Research Laboratory, Wright-Patterson Air Force Base, Dayton, OH 45433, USA

ABSTRACT: We observed the lowest HOMO–LUMO energy transition estimated to be only 1.06 eV for the full-cage shaped emerald-green fullerene EF-6MC$_{4t}$. This energy value was derived from the intercept of characteristic double absorption bands at 1014 (1.23 eV) and 1084 nm (1.14 eV) in the NIR spectrum and the first fluorescence emission band centered at 1278 nm (0.97 eV).

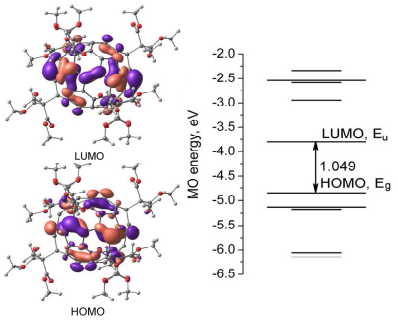

Keywords: 18π-trannulene, emerald-green fullerene, HOMO−LUMO transition, near-IR absorption, low energy gap

Emerald-green fullerenes (EFs) are nanocarbon cage materials exhibiting optical absorption in the near-IR range with their unique intrinsic green color arising from the local belt ring structure in the 18π-trannulenyl electronic configuration located at the equatorial region of the fullerene cage. Three types of EF structures have been explored, namely, polyfluorinated $C_{60}F_{15}$[-$CBr(CO_2Et)_2]_3$ **1**,[1-4] polychlorinated D_{3d}-$C_{60}Cl_{30}$ **2**,[5-7] and the full-cage shaped hexamalonated D_{3d}-C_{60}[-$C(CH_3)(CO_2R)_2]_6$ **3**-C_n (EF-6MC$_n$),[8-11] where R = Me, Et, or *t*-Bu. Among them, EF-6MC$_n$ displayed the longest strong NIR absorption with λ_{max} centered at 762 ($\varepsilon = 6.63 \times 10^3$) and 853 nm ($\varepsilon = 1.28 \times 10^4$ L/mol-cm with the shoulder extending beyond 940 nm) as compared with those of polyfluorinated C_{60} **1** at 612 ($\varepsilon = 8.0 \times 10^3$) and 666 nm ($\varepsilon = 1.05 \times 10^4$ L/mol-cm)[4] and polychlorinated C_{60} **2** at 507 ($\varepsilon = 1.65 \times 10^4$), 511 ($\varepsilon = 1.10 \times 10^4$), and 531 nm ($\varepsilon = 1.30 \times 10^4$ L/mol-cm).[12] These bands were recognized to be associated with the all-*trans*-18π-electrons

conjugated trannulene belt. In the case of EF-6MC$_n$, the belt is interconnected with two triphenylene moieties by one at each side of the belt, as shown in the Schlegel diagram of Figure 1, that composes as the main chromophore structure moieties in the heptad. Synthetically, EF **3**-C$_n$ can be prepared from hexaanionic C$_{60}$ (C$_{60}^{6-}$) in an efficient one-pot reaction from C$_{60}$ at room temperature in a gram-quantity.[8] Here, we report the unique ultra-low 18π-trannulenyl HOMO–LUMO energy gap of EF-6MC$_{4t}$ (**3**-C$_{4t}$) associated with sharp weak absorption features detected at 1014 and 1084 nm in its UV-vis-NIR spectrum (Figure 2).

The lowest energy band gap of **3**-C$_n$ can be elucidated by its fluorescent emission profiles. Several near-IR fluorescence spectra of the solid EF-6MC$_{4t}$ and of its CH_2Cl_2 solution were studied using a 1064 nm laser excitation at the energy level slightly higher than those of low-energy absorption bands. Interestingly, both solution and solid state fluorescence spectra were found to superimpose with each other, as shown in the low-energy part of the spectra in Figure 2, confirming the intrinsic NIR emission nature of **3**-C$_{4t}$. Two main band features in the spectra were observed with a higher peak intensity centered at 1278 nm and a group of peaks centered around 1400 nm [the values for EF-6MC$_2$ (**3**-C$_2$, R = Et) and EF-6MC$_1$ (**3**-C$_1$, R = Me) are almost the same within 100 cm^{-1}]. These two emission peak groups may correspond to two low-energy absorption peaks in the spectra. From their intercept, the energy of the lowest energy transition was estimated to be only 1.06 eV, as compared with that (1.8 eV) of the fullerene monoadduct [6,6]-phenyl-C$_{61}$-butyric acid methyl ester (PCBM), commonly used as the electron-acceptor and -transport component of organic photovoltaic devices.[13]

FT-IR spectra of three EF-6MC$_n$ derivatives are depicted in Figure 3 showing rather similar features in characteristic vibrational absorption peak profiles with each other. DFT calculations[5] predict that IR intensities of all fullerene cage modes are much lower than those for vibrations of 2-methylmalonate addends, leading to the dominance of the latter moieties. Evidently, a good agreement of peak profiles between the experimental spectrum (Figures 3a–c) and the computed spectrum (Figure 3d) derived from the structure of EF-6MC$_1$ were found. Detailed analysis of characteristic group frequencies enabled us to interpret all major absorption bands. The strongest band centered at 1737 cm^{-1} in the spectra of all compounds is readily assigned to the stretching vibrations of C=O bonds. Anti-symmetric deformations of CH_3 groups and scissor vibrations of CH_2 groups appeared as medium intensity bands centered around 1450 cm^{-1}, while symmetric deformations of CH_3 groups exhibited the absorption around 1370 cm^{-1}. A strong broad band at 1260 cm^{-1} was assigned to the asymmetric stretching vibrations of C–C(=O)–O moieties [*i.e.* mixed stretching vibrations of C(=O)–O and (CH_3)C–C(=O)], while the strong band centered at 1120 cm^{-1} is arising from the C(C$_{60}$)–C–C(=O) deformations, rocking CH_3 vibrations, and C–O–R (R = CH_3, C_2H_5, or *t*-Bu) stretching vibrations. Fullerene cage vibrations could be observed only as weak absorptions at 1333, 710, and 552 cm^{-1}.

For the complementary comparison with Figure 3, Raman spectra of EF-6MC$_n$ (Figure 4) were collected using the laser excitation wavelength at 488 nm. Similar spectra were also recorded with the excitation at 514 nm, except for the higher relative intensity of the line at 1440 cm^{-1}. As a result, the strongest line at 1440 cm^{-1} of Figures 4a–c can be tentatively assigned to the stretching vibration of the 18π-trannulene belt that represents a 66 cm^{-1} shift from the analogous vibration in D_{3d}-$C_{60}Cl_{30}$ observed at 1506 cm^{-1}.[12] Resonance character of the spectra excited in the visible range did not allow us to perform the detailed assignment based on the computed off-resonance spectra. A nearly identical spectral pattern (Figures. 4a–c) for all three derivatives having different 2-methylmalonate addend groups indicated that the spectra are mostly originated from the fullerene cage modes. This is in line with the high Raman activity of cage vibrations in C_{60} derivatives.

To clarify the peculiarity of absorption and fluorescence spectra, we have performed DFT quantum-chemical calculations[14,15] of the electronic structure based on the structure of EF-6MC$_{4t}$. The results were visualized in Fig. 5 showing the highest occupied and lowest unoccupied molecular orbitals (HOMO and LUMO) of the molecule, as computed at the PBE/TZ2P level, with the electronic MO energy levels depicted. Frontier orbitals of the molecule are largely localized on the trannulene belt, however, the contribution of triphenylene units is also considerable. This implied that electronic excitations in **3** cannot be modeled by excitations in the trannulene unit alone and are strongly influenced by interactions with remaining parts of the molecule. DFT predicts the HOMO–LUMO energy gap of 1.049 eV in an excellent agreement with the experimental data (1.06 eV). Calculations also revealed that both HOMO and LUMO are two-fold degenerated (E_g and E_u symmetry types, respectively). Based on the D_{3d} molecular symmetry of EF-6MC$_n$, three possible excited states, A_{1u} + A_{2u} + E_u, may be elucidated for HOMO–LUMO transitions, where $S_0 \rightarrow {}^1A_{2u}(1)$ and $S_0 \rightarrow {}^1E_u(1)$ transitions are dipole-allowed and can be assigned to the absorption bands of **3**-C_{4t} detected at 762 and 853 nm (Fig. 2). On the contrary, $S_0 \rightarrow {}^1A_{1u}(1)$ transition is dipole forbidden. Based on these data, we assigned the lowest energy excited state of EF-6MC$_{4t}$ to the ${}^1A_{1u}(1)$ state which implies that vibronic features in the experimental spectra are originated from vibrations of A_{2g} and E_g symmetry types (direct products of these symmetry types with A_{1u} give A_{2u} and E_u, respectively). This assignment agrees with the time-dependent DFT calculation for the isostructural $C_{60}H_6$, which showed ${}^1A_{1u}(1)$ as the lowest energy singlet excited state, followed by ${}^1E_u(1)$ and ${}^1A_{2u}(1)$ excited states.[12] Accordingly, we propose that characteristic low-intensity double absorption bands at 1.23 eV (1014 nm) and 1.14 eV (1084 nm) in the NIR spectrum of **3** and the fluorescence emission bands centered at 1278 nm as lower energy features correspond to the $S_0 \leftrightarrow 1{}^1A_{1u}$ transition, activated by a Herzberg–Theller mechanism through coupling with A_{2g} and E_g vibrational modes. This behavior is reminiscent of

the recently reported calculations for D_{3d}-$C_{60}Cl_{30}$, having a similar trannulene moiety in its structure.[12, 16]

Finally, observed absorption and emission characteristics of the full-cage shaped EF-6MC$_n$ in near-IR wavelengths may facilitate their potential applications as tissue-penetrating NIR bio-imaging agents and as linearly or nonlinearly NIR-photoresponsive, electron-accepting nanomaterials in photovoltaic devices.

■ EXPERIMENTAL METHODS

Synthetic procedure of C_{60}[-C(CH_3)(CO_2-*t*-Bu)$_2$]$_6$ (EF-6MC$_{4t}$)

In a deoxygenated C_{60} (0.40 g, 0.56 mmol) solution in toluene-THF was added sodium naphthalenide solution (10 equiv.) and stirred for a period of 2.0 h at ambient temperature. The resulting blackish suspension was added di-*tert*-butyl-2-bromo-2-methylmalonate (1.3 g, 4.2 mmol) and allowed to react for an additional 12 h at ambient temperature. At the end of the reaction, the greenish brown solution was filtered to separate greyish sodium bromide salt. The solvent was removed from the filtrate to give greenish brown solid residues. The residues were dissolved in a minimum amount of $CHCl_3$ and reprecipitated upon the addition of hexane. The products were then further purified via chromatography (PTLC, SiO_2, R_f = 0.3, THF−toluene/1:9 as eluent) to afford EF-6MC$_{4t}$ as dark green solids in roughly 30% yield and brown solids (R_f = 0.3−0.4, ~35% yield, presumably, a number of combined hexaadduct regioisomers).

Similarly, C_{60}[-C(CH_3)(CO_2Et)$_2$]$_6$ (EF-6MC$_2$) was obtained by the identical synthetic procedure in a comparable yield by quenching C_{60}^{6-} intermediate with diethyl 2-bromo-2-methylmalonate.

Spectroscopic data of EF-6MC$_{4t}$: FT-IR (KBr) ν_{max} 2977 (m), 2931 (w), 1731 (s, C=O), 1632 (w), 1456 (m), 1386 (m), 1368 (m), 1279 (s), 1250 (s), 1173 (s), 1140 (s), 872 (w), 842 (m), 751 (w), 653, and 546 (w) cm^{-1}; UV-vis (THF, 1.0 × 10^{-5} mol/L) λ_{max} (ε) 359 (3.3 × 10^4), 762 (6.2 × 10^3), 852 (1.1 × 10^4), 988 (5.3 × 10^2), 1014 (7.7 × 10^2), 1054 (3.3 × 10^2), 1084 (6.5 × 10^2), and 1114 (2.0 × 10^2) nm; Fluorescence (THF, λ_{ex} 359 nm, 1.0 × 10^{-4} mol/L) λ_{max} 425 and 485 nm; Fluorescence (CH_2Cl_2 and solid, λ_{ex} 1064 nm) λ_{max} 1278 and 1300−1500 (multiple bands) nm; ^{1}H NMR (400 MHz, $CDCl_3$, ppm) δ 1.925 (s, 18H) and 1.542 (s, 108H); ^{13}C NMR (100 MHz, $CDCl_3$, ppm) δ 168.85, 156.35, 146.38, 142.76, 131.01, 82.24, 61.43, 57.13, 28.07, and 20.38.

NIR-fluorescence spectra were measured using EQUINOX-55S FT-IR spectrometer (Bruker, Germany) equipped with Raman attachment FRA-106 and Nd:YAG laser (λ = 1064 nm). The same spectrometer was used for the measurement of IR spectra. Raman spectra were recorded at the room temperature on a T 64000 triple spectrometer (Jobin Yvon, France) with visible laser radiation (Innova 300 series, Coherent, USA) and an excitation wavelength of 488 nm.

■ AUTHOR INFORMATION

Corresponding Authors

*E-mail: a.popov@ifw-dresden.de; popov@phys.chem.msu.ru. Tel: +49 351 465-96-58; E-mail: Long_Chiang@uml.edu. Tel: +1 978-934-3663.

■ ACKNOWLEDGMENT

The authors at UML thank the financial support of Air Force Office of Scientific Research (AFOSR) under the grant numbers FA9550-09-1-0380 and FA9550-09-1-0183. Computer time on "Chebyshev-SKIF" supercomputer in Moscow State University is gratefully acknowledged.

■ REFERENCES

(1) Wei, X.-W.; Darwish, A. D.; Boltalina, O. V.; Hitchcock, P. B.; Street, J. M.; Taylor, R. The Remarkable Stable Emerald Green $C_{60}F_{15}[CBr(CO_2Et)_2]_3$: the First [60]Fullerene That Is also the First [18]Trannulene. *Angew. Chem., Int. Ed.* **2001**, *40*, 2989-2992.

(2) Burley, G. A.; Fowler, P. W.; Soncini, A.; Sandall, J. P. B.; Taylor, R. A Diatropic Rring Current in a Fluorofullerene Ttrannulene. *Chem. Commun.* **2003**, 3042-3043.

(3) Burley, G. A.; Avent, A. G.; Gol'dt, I. V. ; Hitchcock, P. B.; Al-Matar, H.; Paolucci, D.; Paolucci, F.; Fowler, P. W.; Soncini, A.; Street, J. M., *et al*. Design and Synthesis of Multi-Component 18π Annulenic Fluorofullerene Ensembles Suitable for Donor–Acceptor Application. *Org. Biomol. Chem.* **2004**, *2*, 319-329.

(4) Troshin, P. A.; Khakina, E. A.; Zhilenkov, A. V.; Peregudov, A. S.; Troshina, O. A.; Kozlovskii, V. I.; Polyakova, N. V.; Lyubovskaya, R. N. Synthesis and Spectroscopic Characterization of the First Symmetrically and Nonsymmetrically Substituted Fluorinated Emerald-Green Trannulenes $C_{60}F_{15}R_3$ Soluble in Polar Media and Water. *Eur. J. Org. Chem.* **2010**, 1037-1045.

(5) Troyanov, S. I.; Kemnitz, E. Synthesis and Structures of Fullerene Bromides and Chlorides. *Eur. J. Org. Chem.* **2005**, 4951-4962.

(6) Troyanov, S. I.; Shustova, N. B.; Popov, A. A.; Sidorov, L. N. Synthesis and Structures of C_{60} Fullerene Chlorides. *Russ. Chem. Bull., Int. Ed.* **2005**, *7*, 1656-1666.

(7) Troshin, P. A.; Lyubovskaya, R. N.; Ioffe, I. N.; Shustova, N. B.; Kemnitz, E.; Troyanov, S. I. Synthesis and Structure of the Highly Chlorinated [60]Fullerene $C_{60}Cl_{30}$ with a Drum-Shaped Carbon Cage. *Angew. Chem., Int. Ed.* **2005**, *44*, 234-237.

(8) Canteenwala, T.; Padmawar, P. A.; Chiang, L. Y. Intense Near-Infrared Optical Absorbing Emerald Green [60]Fullerenes. *J. Am. Chem. Soc*. **2005**, *127*, 26-27.

(9) Canteenwala, T.; Wang, H.-L.; Chiang, L. Y. Low Electron Reduction Potentials of Ethylated Emerald Green [60]Fullerene, *Chem Lett*. **2006**, *35*, 762-763.

(10) El-Khouly, M. E.; Canteenwala, T.; Araki, Y.; Ito, O.; Chiang, L. Y. Unusual Photophysical Properties of Emerald Green [60]Fullerenes and Its Charge Complexes, *Chem Lett*. **2006**, *35*, 710-711.

(11) Kokubo, K.; Arastoo, R.; Oshima, T.; Wang, C.-C.; Gao, Y.; Wang, H.-L.; Geng, H.; Chiang, L. Y. Synthesis and Regiochemistry of [60]Fullerenyl 2-Methylmalonate Bisadducts and their Facile Electron-Accepting Properties. *J. Org. Chem*. **2010**, *75*, 4574-4583.

(12) Popov, A. A.; Senyavin, V. M.; Troyanov, S. I**.** Electronic Structure **a**nd Spectroscopic Studies of D_{3d}-$C_{60}Cl_{30}$, a Chlorofullerene with a [18]Trannulene Ring, and Its Relation to Other [18]Trannulenes. *J. Phys. Chem. A* **2006**, *110*, 7414-7421.

(13) Kim, J. Y.; Lee, K.; Coates, N. E.; Moses, D.; Nguyen, T.-Q.; Dante, M.; Heeger, A. J. Efficient Tandem Polymer Solar Cells Fabricated by All-Solution Processing. *Science* **2007**, *317*, 222-225.

(14) DFT quantum-chemical calculations were performed with the PRIRODA package[15] using PBE functional and implemented TZ2P-quality basis set.

(15) Laikov, D. N.; Ustynuk, Y. A. A Quantum-Chemical Program Suite. New Possibilities in the Study of Molecular Systems with the Application of Parallel Computing. *Russ. Chem. Bull.* **2005**, *54*, 820-826.

(16) Korepanov, V. G.; Popov, A. A.; Senyavin, V. M.; Troyanov, S. I.; Razbirin, B. S.; Ovchinnikova, N.; Yurovskaya, M.; Starukhin, A. Vibrational Structure in the Electronic Spectra of C_{60} and Fullerene Derivatives as Studied by Time-Dependent Density Functional Theory. *ECS Transactions* **2006**, *2* (12), 121-132.

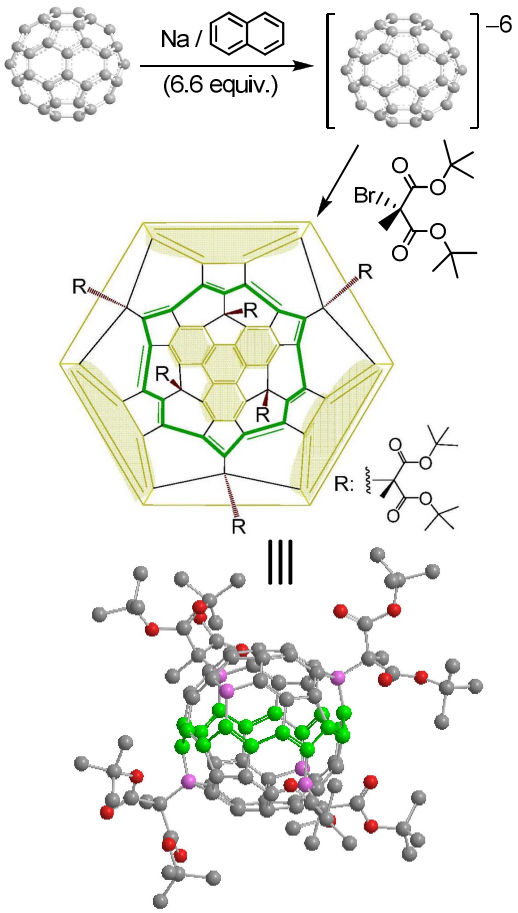

Figure 1. Synthesis and a Schlegel diagram of the full-cage shaped EF-6MC$_{4t}$ (**3**-C$_{4t}$) showing all-*trans*-18π-trannulene belt (green lines) and interconnected two triphenylene moieties (yellow shadow).

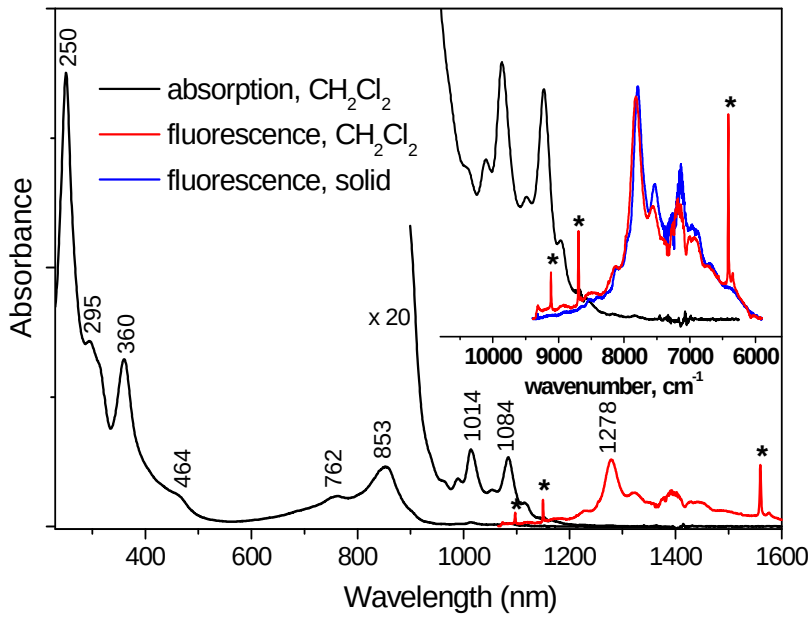

Figure 2. Absorption and fluorescence (excitation by Nd-YAG laser at 1064 nm) spectra of EF-6MC$_{4t}$. Sharp peaks marked by asterisks in solution fluorescence spectrum are Raman lines of CH_2Cl_2. Inset shows an enhanced region of the absorption and fluorescence spectra in the vicinity of their crossing; for the sake of comparison, the scale in the inset is given in cm^{-1} as these units are directly proportional to energy.

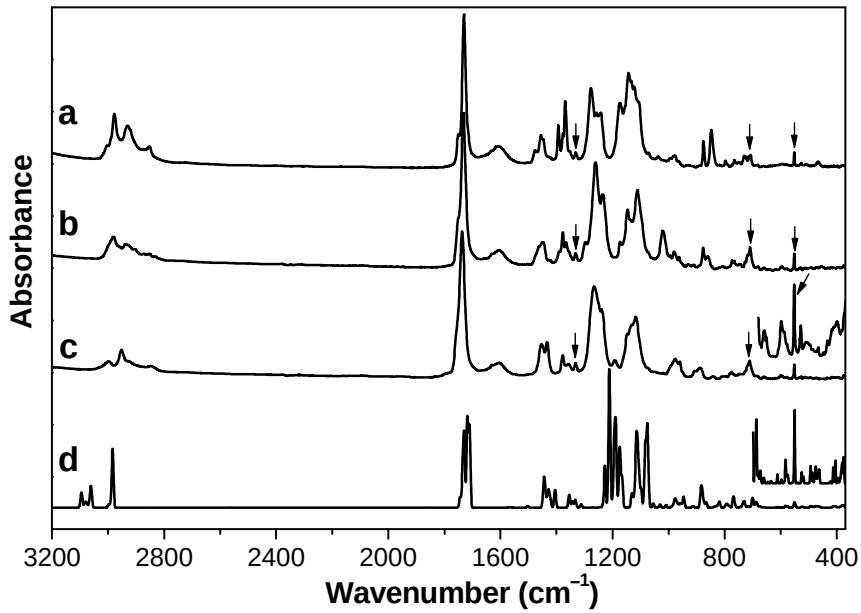

Figure 3. FTIR spectra of (a) EF-6MC$_{4t}$, (b) EF-6MC$_2$, (c) EF-6MC$_1$, and (d) calculated spectrum of EF-6MC$_1$. The arrows denote cage vibrations.

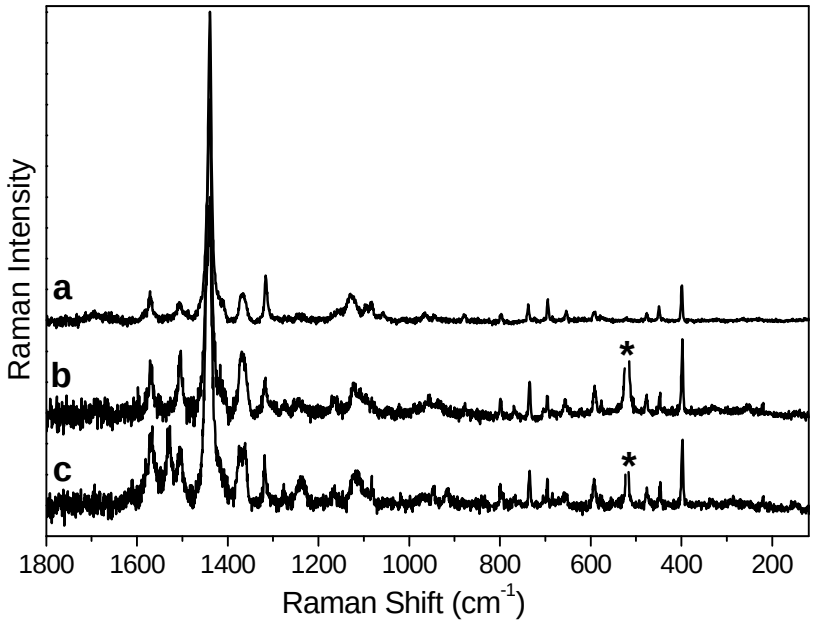

Figure 4. Raman spectra (excitation wavelength of 488 nm) of (a) EF-6MC$_{4t}$, (b) EF-6MC$_2$, and (c) EF-6MC$_1$. The asterisks denote Raman line of Si substrate at 520 cm^{-1}.

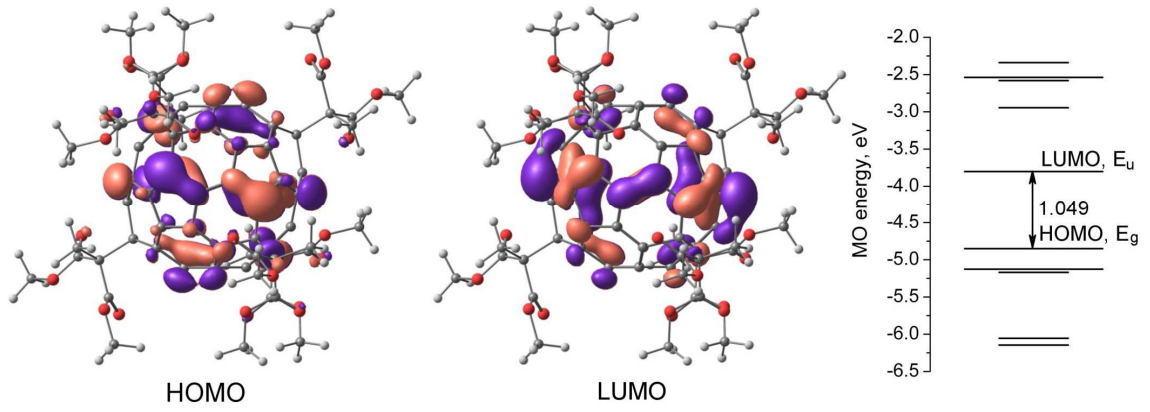

Figure 5. DFT-computed frontier orbitals and MO energy levels in EF-6MC$_{4t}$.